Monthly Notices
of the
ROYAL ASTRONOMICAL SOCIETY

MNRAS **460**, 2376–2384 (2016) doi:10.1093/mnras/stw1067
Advance Access publication 2016 May 5

Radio Galaxy Zoo: discovery of a poor cluster through a giant wide-angle tail radio galaxy

J. K. Banfield,[1,2★] H. Andernach,[3★] A. D. Kapińska,[2,4] L. Rudnick,[5] M. J. Hardcastle,[6] G. Cotter,[7] S. Vaughan,[7] T. W. Jones,[5] I. Heywood,[8,9] J. D. Wing,[10] O. I. Wong,[2,4] T. Matorny,[11] I. A. Terentev,[11] Á. R. López-Sánchez,[12,13] R. P. Norris,[8,14] N. Seymour,[15] S. S. Shabala[16] and K. W. Willett[5]

[1] *Research School of Astronomy and Astrophysics, Australian National University, Canberra, ACT 2611, Australia*
[2] *ARC Centre of Excellence for All-Sky Astrophysics (CAASTRO)*
[3] *Departamento de Astronomía, DCNE, Universidad de Guanajuato, Apdo. Postal 144, CP 36000 Guanajuato, Gto., Mexico*
[4] *International Centre for Radio Astronomy Research-M468, The University of Western Australia, 35 Stirling Hwy, Crawley, WA 6009, Australia*
[5] *School of Physics and Astronomy, University of Minnesota, 116 Church St. SE, Minneapolis, MN 55455, USA*
[6] *Centre for Astrophysics Research, School of Physics, Astronomy and Mathematics, University of Hertfordshire, College Lane, Hatfield AL10 9AB, UK*
[7] *Oxford Astrophysics, Denys Wilkinson Building, Keble Road, Oxford OX1 3RH, UK*
[8] *CSIRO Astronomy and Space Science, Australia Telescope National Facility, PO Box 76, Epping, NSW 1710, Australia*
[9] *Department of Physics and Electronics, Rhodes University, PO Box 94, Grahamstown 6140, South Africa*
[10] *Harvard-Smithsonian Center for Astrophysics, 60 Garden St., Cambridge, MA 02138, USA*
[11] *Zooniverse Citizen Scientist, c/o Oxford Astrophysics, Denys Wilkinson Building, Keble Road, Oxford OX1 3RH, UK*
[12] *Australian Astronomical Observatory, PO Box 915, North Ryde, NSW 1670, Australia*
[13] *Department of Physics and Astronomy, Macquarie University, NSW 2109, Australia*
[14] *Western Sydney University, Locked Bag 1797, Penrith South, NSW 1797, Australia*
[15] *International Centre for Radio Astronomy Research, Curtin University, Perth, WA 6102, Australia*
[16] *School of Physical Sciences, University of Tasmania, Private Bag 37, Hobart, TAS 7001, Australia*

Accepted 2016 May 2. Received 2016 March 9

ABSTRACT

We have discovered a previously unreported poor cluster of galaxies (RGZ-CL J0823.2+0333) through an unusual giant wide-angle tail radio galaxy found in the Radio Galaxy Zoo project. We obtained a spectroscopic redshift of $z = 0.0897$ for the E0-type host galaxy, 2MASX J08231289+0333016, leading to $M_{\rm r} = -22.6$ and a 1.4 GHz radio luminosity density of $L_{1.4} = 5.5 \times 10^{24}$ W Hz^{-1}. These radio and optical luminosities are typical for wide-angle tailed radio galaxies near the borderline between Fanaroff–Riley classes I and II. The projected largest angular size of ≈8 arcmin corresponds to 800 kpc and the full length of the source along the curved jets/trails is 1.1 Mpc in projection. X-ray data from the *XMM–Newton* archive yield an upper limit on the X-ray luminosity of the thermal emission surrounding RGZ J082312.9+033301 at 1.2–2.6 × 10^{43} erg s^{-1} for assumed intracluster medium temperatures of 1.0–5.0 keV. Our analysis of the environment surrounding RGZ J082312.9+033301 indicates that RGZ J082312.9+033301 lies within a poor cluster. The observed radio morphology suggests that (a) the host galaxy is moving at a significant velocity with respect to an ambient medium like that of at least a poor cluster, and that (b) the source may have had two ignition events of the active galactic nucleus with 10^7 yr in between. This reinforces the idea that an association between RGZ J082312.9+033301 and the newly discovered poor cluster exists.

Key words: galaxies: active – galaxies: clusters: individual: RGZ J082312.9+033301 – radio continuum: galaxies.

1 INTRODUCTION

High-resolution radio surveys performed over the past decades have shown the wide variety of radio morphologies of galaxies

★E-mail: julie.banfield@anu.edu.au (JKB); heinz@astro.ugto.mx (HA)

illustrating the complexity of the underlying physics. The majority of radio sources have compact morphology (Shabala et al. 2008; Sadler et al. 2014) while the extended radio-loud sources tend to be Fanaroff–Riley (FR) types I and II (Fanaroff & Riley 1974). However, there are some extended radio-loud sources that do not fit the standard FR I or FR II classification.

The division of tailed radio galaxies into narrow-angle tails (NATs, head) and wide-angle tails (WATs) was introduced by Owen & Rudnick (1976) and Rudnick & Owen (1976). Tailed radio galaxies have provided evidence that in both dense and sparse environments, the bending and distortions of radio galaxies are the result of motions with respect to the thermal plasma. WATs and straight FR I sources are often associated with the brightest galaxies in clusters (BCGs). Their radio morphologies reflect both the initial jet momentum and the mild effects of motions (e.g. Coziol et al. 2009 have shown that a large number of BCGs have a significant peculiar velocity compared to their cluster mean) and pressure gradients in the intracluster medium (ICM; Pinkney, Burns & Hill 1994; Giacintucci & Venturi 2009).

WATs generally have C-shaped morphologies and have radio luminosities near the FR I and FR II luminosity transition (Owen & Ledlow 1994). WATs are found in both merging and relaxed clusters at, or near, the centre and display highly collimated jets. Early models of WATs suggested that ICM ram pressure resulting from velocities $>1000\,\mathrm{km\ s^{-1}}$ was required to produce the observed bends (Eilek et al. 1984; O'Donoghue, Eilek & Owen 1993) but models using light jets by Sakelliou, Merrifield & McHardy (1996), Hardcastle, Sakelliou & Worrall (2005), Jetha, Hardcastle & Sakelliou (2006), and Mendygral, Jones & Dolag (2012) show that bulk velocities around $100\,\mathrm{km\ s^{-1}}$ are sufficient to produce WATs.

FR II radio sources have their size and shape dominated by the momentum of the overpressured jet. As the jet expands it develops a cocoon and a more collimated jet flows out to power the hotspots. The jets in FR I-NATs undergo a complete disruption, after which they are carried back by external motions alone with no surrounding cocoon. Intermediate between these extremes, FR I-WATs and straight FR Is have cocoons surrounding the outer portions of their jets (Hardcastle 1998; Katz-Stone et al. 1999), so both jet momentum and motions in the surrounding thermal medium influence the subsequent flow.

Questions remain unanswered from both the models and the observations. Are any bright radio spots or knots in the jets powered by an impinging jet? Has the energy supply shut off, so that the knots are in the process of fading due to radiative losses and mechanical dissipation? Is the jet outflow exposed to the external plasma or shielded by a stationary or slower moving cocoon of relativistic plasma as observed around FR II and some FR I jets?

The Radio Galaxy Zoo discovery of a giant WAT (RGZ J082312.9+033301) shows the power of using bent radio sources as tracers of clusters. Upcoming wide-area radio surveys the Evolutionary Map of the Universe (EMU; Norris et al. 2011), the Westerbork Observations of the Deep APERTIF Northern sky (WODAN) survey (Röttgering et al. 2011), and the deeper radio survey MeerKAT International GigaHertz Tiered Extragalactic Exploration (MIGHTEE) survey (Jarvis 2012) are expected to detect over 100 000 bent radio sources (Norris et al. 2011). Radio Galaxy Zoo will allow us to locate these bent radio sources and to investigate the physics that allows jets to be tightly collimated while undergoing significant bending.

The present paper is organized as follows. Section 2 describes the discovery of the WAT while in Section 3 we discuss the

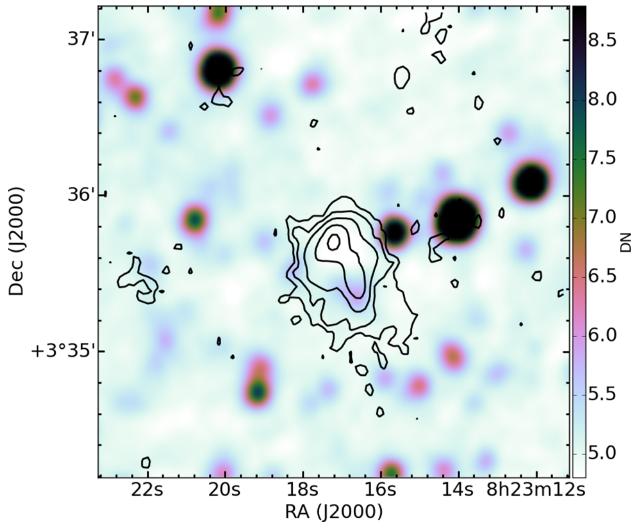

Figure 1. The Radio Galaxy Zoo 3 × 3 arcmin^2 cut-out of the FIRST radio data (black contours) with the *WISE* 3.4 μm image (grey-scale) of the Radio Galaxy Zoo subject FIRST J082317.2+033542 that first indicated a possible larger object shown in Fig. 2. The contours start at two times the local signal-to-noise ratio ($1\sigma = 0.19\,\mathrm{mJy\ beam^{-1}}$) and increase by multiples of 2. The background colour scheme comes from CUBEHELIX (Green 2011). A colour version of the figure is available in the online version.

implications with respect to environment, dynamics, and the central active galactic nucleus (AGN). Section 4 presents our conclusions. Throughout this paper we adopt a Λ cold dark matter (ΛCDM) cosmology of $\Omega_\mathrm{M} = 0.3, \Omega_\Lambda = 0.7$ with a Hubble constant of $H_0 = 70\,\mathrm{km\ s^{-1}\ Mpc^{-1}}$. With $z = 0.0897$, the luminosity distance is $D_L = 410$ Mpc and the angular size distance is $D_\mathrm{A} = 345.3$ Mpc giving a scale of 1.674 kpc arcsec^{-1} (Wright 2006). We define the radio spectral index as $S_\nu \propto \nu^\alpha$.

2 WIDE ANGLE TAIL RGZ J082312.9+033301

The discovery of RGZ J082312.9+033301 was made in the citizen science project Radio Galaxy Zoo[1] (Banfield et al. 2015). Radio Galaxy Zoo offers overlays of the 3.4 μm image from the *Wide-Field Infrared Survey Explorer* (*WISE*; Wright et al. 2010) with the 1.4 GHz image from the Faint Images of the Radio Sky at Twenty cm (FIRST; Becker, White & Helfand 1995; White et al. 1997). The 3 × 3 arcmin^2 Radio Galaxy Zoo images are centred on the position of the radio sources listed as extended in the FIRST catalogue (version 14 March 2004) and then overlaid on the infrared image as we show in Fig. 1. The radio images are illustrated with radio brightness contours, overlaid on a *WISE* 3.4 μm image in a heat scale.

RGZ J082312+033301 was identified as an unusual object in 2013 December by two citizen scientists (T. Matorny and I. Terentev) after examining the Radio Galaxy Zoo 3 × 3 arcmin^2 cut-out (Fig. 1) of a section of the radio galaxy (N2 in Fig. 2). Matorny first suggested that the radio emission pointed towards another object by way of the radio extension towards the south-west. A further investigation of RGZ J082312+033301 by Terentev and Rudnick was completed in RadioTalk[2] by examining the larger cut-out of both the FIRST and *WISE* images along with images from the NRAO

[1] http://radio.galaxyzoo.org
[2] http://radiotalk.galaxyzoo.org

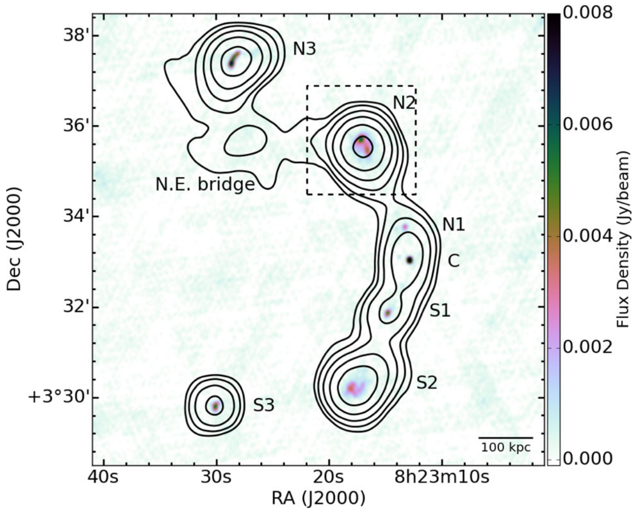

Figure 2. The 1.4 GHz FIRST radio image (grey-scale) with the 1.4 GHz NVSS contours shown in black. Contour levels begin at two times the local signal-to-noise ratio level ($1\sigma = 0.83$ mJy beam^{-1}) and increase by a factor of 2. The components of RGZ J082321+033301 are labelled (clockwise from N.E.). The dashed square indicates the area covered by the Radio Galaxy Zoo image from Fig. 1. A colour version of the figure is available in the online version.

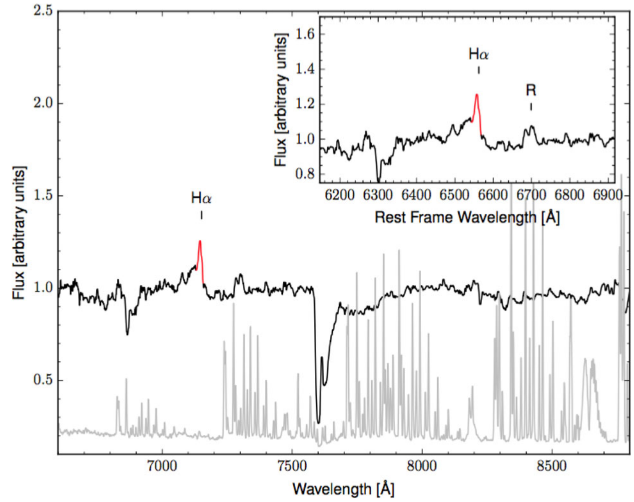

Figure 3. The Oxford SWIFT IFU spectrum (black lines) of 2MASX J08231289+0333016 with the skylines (grey lines). The inset zooms into the region of the most important lines (Hα, [N II] λ6583, or [S II] $\lambda\lambda$6716, 6731). The redshifted Hα line provides a redshift of $z = 0.0897 \pm 0.0001$. Note that the features near the expected position of the [S II] doublet (expected wavelength marked) are the skyline residuals. A colour version of the figure is available in the online version.

VLA Sky Survey (NVSS; Condon et al. 1998) and the Sloan Digital Sky Survey (SDSS) Data Release 10 (DR10; Ahn et al. 2014) and Data Release 12 (DR12; Alam et al. 2015). It was then realized that the isolated component seen in Fig. 1 was part of a much more extended radio source which could be classified as a WAT.

In Fig. 2 we show the FIRST image in a colour scale and the NVSS image with contours. We found that the core (C in Fig. 2) is coincident with 2MASX J08231289+0333016 (SDSS J082312.91+033301.3) and has 175 morphology votes from Galaxy Zoo 2 (Willett et al. 2013) indicating that the host galaxy has morphological features consistent with type E0 with $M_{\rm r} = -22.6$ and $M_V = -22.3$. There is no spectrum of SDSS J082312.91+033301.3 in SDSS DR12. We used the Oxford Short Wavelength Integral Field Spectrograph for Large Telescopes (SWIFT) Integral Field Unit (IFU) spectrograph (Thatte et al. 2010) on the Palomar 5-m Hale telescope to obtain an optical spectrum of SDSS J082312.91+033301.3 on the night of 2013 December 29 UT. The target was observed with the large (0.235 arcsec) plate scale in natural seeing. We took two 300-s exposures, offset from each other by 40 arcsec along the long axis of the detector to allow background subtraction. We present the one-dimensional spectrum, extracted from a 7-arcsec diameter circular aperture, in Fig. 3.

Only one secure non-telluric feature is detected in this spectrum: a narrow line centred at 7151.18 Å. We identify the line as Hα (rest wavelength of 6562.81 Å), providing a redshift of $z = 0.0897 \pm 0.0001$. The uncertainty in the redshift is dominated by the subjective choice of baseline when fitting the continuum level interactively in the IRAF software; the intrinsic resolution of the spectrograph is $R \approx 4000$. We note that there is no clear evidence for [N II] λ6583 or [S II] $\lambda\lambda$6716, 6731emission.

Archival Very Large Array (VLA) data at 8 GHz (project ID AM0593) allow us to determine that the core ($S_{8.4} = 12.6 \pm 0.2$ mJy) is a flat-spectrum object with $\alpha = -0.10 \pm 0.01$. Table 1 lists the possible components of RGZ J082312.9+033301 and the corresponding NVSS and FIRST identifications. Using radio components S2 to N3, we estimate the luminosity density to be $L_{1.4} = 5.5 \times 10^{24}$ W Hz^{-1}. This places RGZ J082312.9+033301 below the FR I/FR II boundary in a radio versus optical luminosity diagram like fig. 4 of Best (2009). However, RGZ J082312.9+033301 is still inside the rectangular area where FR Is and FR IIs occur with almost equal frequency, making it an analogue of local FR I radio galaxies like 3C 31. The lack of strong lines in the spectrum suggests that RGZ J082312.9+033301 is a low-excitation radio galaxy (LERG).

The northern section of the radio complex is marked with the labels N1, N2, N3, and N.E. bridge in Fig. 2. In Fig. 4(a) we show the diffuse emission connecting components N2–N3. The N.E. bridge is detected in the lower resolution NVSS image at a peak brightness of ≈4 mJy beam^{-1} with a total flux density of 23 mJy spread over five NVSS beams, and is not detected in FIRST. We note that N3 may originate from a faint galaxy SDSS J082328.28+033733.2 (Fig. 4b) at a spectroscopic redshift of $z = 0.2601$ (Adelman-McCarthy et al. 2006). Deeper radio observations are required to determine if component N3 is connected to the rest of RGZ J082312.9+033301.

Given the presently available data, there is no hint of diffuse emission connecting components S2 and S3. However, preliminary analysis of the radio structure from DnC configuration Karl G. Jansky VLA observations (Heywood et al., in preparation) indicate a diffuse radio structure to the south of S2 as marginally detected in the NVSS data (Fig. 5). This structure is not included in the analysis of this current work. The WAT has a projected largest angular size (LAS) of ≈8 arcmin, corresponding to 800 kpc, and the total length along the curved ridge of jets/trails is ≈1.1 Mpc in projection. This makes this WAT comparable in size to 4C+47.51, which, to our knowledge, is still the largest WAT reported by Pinkney et al. (1994).

3 DISCUSSION

3.1 Environment of RGZ J082312+033301

As radio galaxies of WAT morphology tend to trace rich environments, in this section we assess the environment of

Table 1. The identification of the possible seven components of RGZ J082312.9+033301 from the NVSS and FIRST catalogues shown in Fig. 2.

Comp.	RA (J2000) (°)	Dec. (J2000) (°)	FIRST ID	$S_{1.4\,\mathrm{FIRST}}$ (mJy)	NVSS ID	$S_{1.4\,\mathrm{NVSS}}$ (mJy)	Note
N3	125.869	3.623	J082328+033722	15.38	J082328+033724	56.4	Potential component
			J082328+033733	11.56			
N2	125.824	3.593	J082317+033534	12.28	J082317+033530	87.5	
			J082316+033530	36.94			
			J082317+033542	12.71			
N1	125.806	3.563	J082313+033345	6.28	–	–	
C	125.804	3.550	J082312+033301	16.50	J082313+033241	60.3	
S1	125.812	3.531	J082314+033151	10.08	J082314+033047	3.8	
S2	125.822	3.503	J082317+033011	18.26	J082317+033016	71.1	
			J082318+033012	21.33			
			J082317+033006	3.07			
S3	125.875	3.497	J082330+032947	13.65	J082330+032950	16.5	Unlikely component

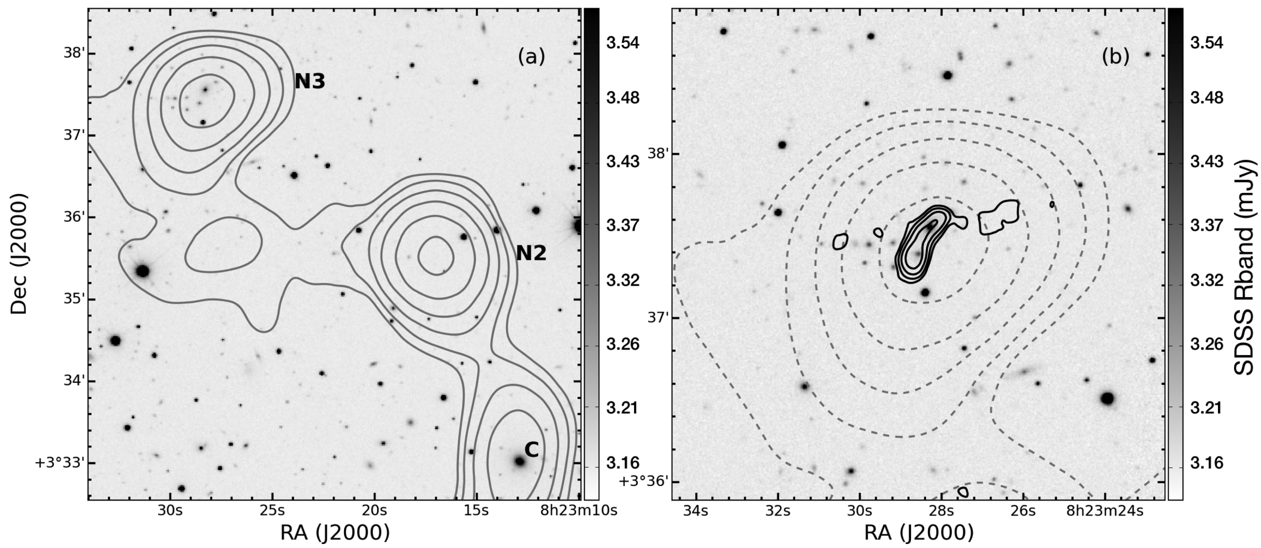

Figure 4. (a) Enlargement of the N.E. bridge along with components C, N2, and N3 from Fig. 2. The SDSS r-band image is shown in the inverted grey-scale and the NVSS data are shown as contours, starting at two times the local noise ($1\sigma = 0.83\,\mathrm{mJy\,beam^{-1}}$) and increasing by a factor of 2. (b) A 3×3 arcmin^2 enlargement of N3 showing the possible alignment of N3 to a background cluster of galaxies at $z = 0.2601$. The NVSS data are shown as grey dashed contours, the FIRST data are shown as black solid contours, and the SDSS r-band image is shown in the inverted grey-scale. The FIRST contours start at two times the local noise ($1\sigma = 0.19\,\mathrm{mJy\,beam^{-1}}$) and increasing by a factor of 2.

RGZ J082312.9+033301 using the optical and X-ray data available to us.

3.1.1 Optical galaxy counts

Fig. 5 shows the SDSS colour composite image of the environment surrounding the host galaxy of RGZ J082312.9+033301. The dashed circle represents a radius of 1.0 Mpc. Table 2 lists all of the galaxies within 31 arcmin of RGZ J082312+033301 and with spectroscopically measured redshifts from SDSS DR12 (Alam et al. 2015) in the range $0.08 < z < 0.09$. We found no reported galaxies with a spectroscopic redshift in the range $0.09 < z < 0.10$ within our search radius and none between 0.053 and 0.080 within 20 arcmin radius.

To determine the richness of the cluster environment surrounding RGZ J082312+033301, we use the parameter $N_{1.0}^{-19}$ as described in Wing & Blanton (2011). This is a background subtracted count of all galaxies brighter than $M_{\rm r} = -19$ at the redshift of the radio source and within a radius of 1.0 Mpc around the radio source. The background count rate is determined locally using an annulus centred on the radio source with a radius from 2.7 to 3.0 Mpc. We find RGZ J082312.9+033301 to be located in an environment with $N_{1.0}^{-19} = 42 \pm 1$. This implies that the cluster environment surrounding RGZ J082312.9+033301 is near the poor end of the cluster richness spectrum; the vast majority of Abell clusters analysed by Wing & Blanton (2011) have $N_{1.0}^{-19} > 40$.

However, Rykoff et al. (2014) do not detect a cluster near RGZ J082312.9+033301 in their redMaPPer catalogue. The galaxy group which we propose as a possible counterpart of radio component N3 was identified by Hao et al. (2010) as the brightest galaxy of the cluster GMBCG J125.86785+03.62590 with $z_{\rm phot} = 0.288$, as well as by Rykoff et al. (2014) as the brightest cluster galaxy of redMaPPer cluster RM J082328.3+033733.2 with $z_{\rm phot} = 0.2647$ and richness $=28 \pm 3$ (as of v5.10 of the catalogue).[3] However, the Radio Galaxy Zoo WAT host cluster proposed in the present paper is not listed in this cluster catalogue, possibly indicating that its richness is $\lambda \lesssim 20$.

[3] http://risa.stanford.edu/redmapper

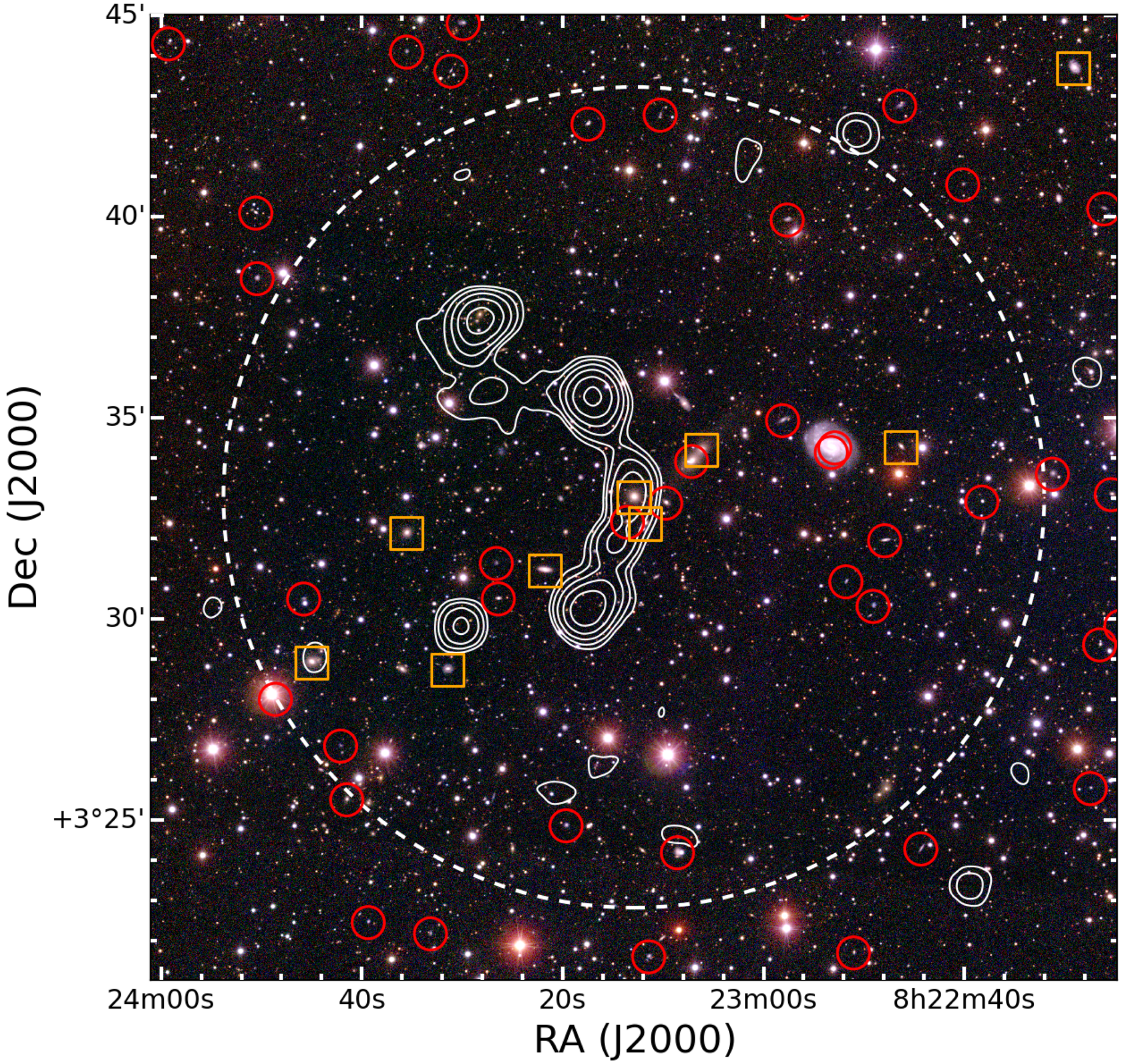

Figure 5. A colour composite of the environment within 1 Mpc (10 arcmin, the radius of the white dashed circle) of RGZ J082312.9+033301. The background is the rgb image of the SDSS field using the i-band image as red (min = −0.002, max = 0.540), green as the r band (min = −0.006, max = 0.710), and the g band for blue (min = −0.002, max = 0.280), all using the asinh stretch (Lupton et al. 2004). The NVSS 1.4-GHz radio flux density is shown with the white contours as displayed in Fig. 2. The orange squares indicate the galaxies with a spectroscopic redshift of $0.08 < z < 0.09$ and the red circles indicate the galaxies with a photometric redshift of $0.05 < z < 0.12$. A colour version of the figure is available in the online version.

3.1.2 Velocity dispersion

The velocity dispersion of the environment gives an indication of its virial mass and therefore of its richness. The radial velocity distribution of the 14 galaxies with spectroscopic redshifts within 20 arcmin (2 Mpc) of RGZ J082312.9+033301 is strongly peaked around 25 000 km s^{-1}. We ran these velocities through the ROBUST software (Beers, Flynn & Gebhardt 1990) to estimate the mean velocity and velocity dispersion, finding $C_{\rm BI} = 25743 \pm 100$ km s^{-1} and $S_{\rm BI} = 373 \pm 65$ km s^{-1}. This velocity dispersion would again be consistent with a rich group or poor cluster of galaxies (e.g. Becker et al. 2007). Interestingly, with a redshift of $z = 0.0897$, RGZ J082312.9+033301 is an outlier in the velocity distribution, with a radial velocity of $cz = 26\,900$ km s^{-1}, so that it has a relative (or 'peculiar') velocity with respect to the 13 remaining galaxies of $(26900 - 25700)/(1 + z) = +1100 \pm 100$ km s^{-1}. We return to this point below, Section 3.2.

3.1.3 X-ray emission

RGZ J082312.9+033301 lies at the extreme edge of an archival *XMM–Newton* data set (Project ID 0721900101). At 14 arcmin from the detector centre, the target is out of the field of view of the two MOS cameras and barely in the pn field of view. The pn data were moderately affected by soft proton flaring and were filtered to an exposure time of 13.8 ks before analysis.

Table 2. The 23 galaxies with a spectroscopic redshift of $0.08 < z < 0.09$ within 31 arcmin of RGZ J082312.9+033301. The table includes the name of the object, position, SDSS r'-band magnitude, spectroscopic, and the distance in arcmin between RGZ J082312.9+033301 and the object. The values are obtained from NED and SDSS DR12 (Alam et al. 2015).

Name	RA (J2000) (°)	Dec. (J2000) (°)	r' (mag)	$z_{\rm spec}$	Separation (arcmin)
RGZ J082312.9+033301	125.80381	+03.55038	15.66 ± 0.01	0.08970 ± 0.00020	0.0
SDSS J082311.78+033222.1	125.79912	+03.53947	17.24 ± 0.01	0.08607 ± 0.00002	0.7
SDSS J082306.16+033412.1	125.77570	+03.57004	16.37 ± 0.01	0.08574 ± 0.00003	2.1
SDSS J082321.81+033112.4	125.84089	+03.52012	15.96 ± 0.01	0.08390 ± 0.00002	2.9
SDSS J082335.54+033207.6	125.89813	+03.53546	16.58 ± 0.01	0.08693 ± 0.00003	5.7
SDSS J082331.46+032844.4	125.88110	+03.47901	16.99 ± 0.01	0.08762 ± 0.00001	6.3
SDSS J082246.34+033416.3	125.69312	+03.57122	19.75 ± 0.02	0.08430 ± 0.00003	6.7
SDSS J082345.00+032855.2	125.93754	+03.48201	16.08 ± 0.01	0.08710 ± 0.00002	9.0
SDSS J082229.09+034341.8	125.62124	+03.72828	16.26 ± 0.01	0.08549 ± 0.00002	15.3
SDSS J082405.88+034419.0	126.02453	+03.73861	17.74 ± 0.01	0.08507 ± 0.00001	17.4
SDSS J082403.25+034601.9	126.01360	+03.76720	17.60 ± 0.01	0.08474 ± 0.00001	18.1
SDSS J082423.97+033958.7	126.09989	+03.66631	16.42 ± 0.01	0.08583 ± 0.00002	19.0
SDSS J082205.11+032332.8	125.52133	+03.39244	17.14 ± 0.01	0.08589 ± 0.00003	19.4
SDSS J082431.70+032859.8	126.13211	+03.48329	17.15 ± 0.01	0.08625 ± 0.00001	20.1
SDSS J082221.02+035201.4	125.58760	+03.86707	17.81 ± 0.01	0.08710 ± 0.00002	23.0
SDSS J082201.96+031805.8	125.50822	+03.30161	16.25 ± 0.01	0.08511 ± 0.00002	23.2
SDSS J082207.20+031422.1	125.53001	+03.23947	16.75 ± 0.01	0.08471 ± 0.00002	24.8
SDSS J082319.91+035915.0	125.83297	+03.98753	16.63 ± 0.01	0.08530 ± 0.00001	26.3
SDSS J082458.64+032903.3	126.24436	+03.48428	15.86 ± 0.01	0.08570 ± 0.00002	26.7
SDSS J082432.04+035246.3	126.13351	+03.87955	19.37 ± 0.02	0.08882 ± 0.00002	27.9
SDSS J082324.85+040213.9	125.85357	+04.03720	17.76 ± 0.01	0.08873 ± 0.00001	29.4
SDSS J082257.82+040227.8	125.74096	+04.04106	16.43 ± 0.01	0.08512 ± 0.00002	29.7
SDSS J082450.69+031331.3	126.21122	+03.22538	16.56 ± 0.01	0.08543 ± 0.00001	31.2

RGZ J082312.9+033301 is clearly detected as a point-like source in the pn data coincident with the radio core (C). In the 0.3–8.0 keV range there are approximately 40 counts after background subtraction in a 30-arcsec radius centred on the detection, just enough to fit a rough spectrum on the assumption of a power-law model with a fixed photon index of 1.8 and Galactic absorption ($N_{\rm H}$ = 3.77 $\times$ 10^{20} cm^{-2}, from COLDEN). This gives a background subtracted 2–10 keV luminosity of $(3 \pm 1) \times 10^{41}$ erg s^{-1}, which is entirely consistent with what we might expect from jet-related emission from the unresolved core, given its 1.4-GHz flux density (Hardcastle, Evans & Croston 2009).

There is no visual evidence for additional thermal X-ray emission directly surrounding RGZ J082312.9+033301, which in itself rules out a rich cluster environment at this redshift. To make this quantitative we measured counts in a 60° pie-slice to the north-east of RGZ J082312.9+033301, excluding the AGN and extending out to an AGN-centric radius of 280 arcsec (480 kpc). We find a 3σ upper limit on the 0.3–8.0 keV counts in this region of 195, leading to a limit on the counts from an assumed circularly symmetric X-ray environment of <1170 counts. The temperature of the non-detected environment is unknown but we convert this limit to a luminosity on the assumption of various temperatures in the range $kT = 1.0$ (appropriate for a reasonably rich group) to 5.0 keV (a rich cluster), assuming 0.3 solar abundance and the redshift of RGZ J082312.9+033301. The bolometric luminosity upper limits implied by this are between 1.2 $\times$ 10^{43} erg s^{-1} for kT = 1.0 keV and 2.6 $\times$ 10^{43} erg s^{-1} for kT = 5.0 keV, which is certainly not consistent with a rich cluster environment given the well-known temperature–luminosity relation for groups and clusters. It is, however, consistent with the measured velocity dispersion: Helsdon & Ponman (2000) find that one may expect a luminosity $\sim 10^{43}$ erg s^{-1} for $S_{\rm BI} \approx 400$ km s^{-1}. We note that this is also the typical luminosity for a low-excitation radio galaxy of this luminosity found in the study of Ineson et al. (2015).

It is worth noting that there is a marginally significant detection of extended emission with 90 ± 30 background subtracted 0.3–8.0 keV counts in a 1-arcmin source circle centred at RA = $08^{\rm h}23^{\rm m}07\overset{\rm s}{.}0$, Dec. = $+03°33'53''$, 1.7 arcmin (170 kpc) to the north-west of RGZ J082312.9+033301. Given the signal-to-noise ratio it is impossible to confirm that this is thermal emission, but it is perfectly possible that it represents the peak of the thermal emission from a group of galaxies with the properties estimated above from the optical data, possibly associated with the bright nearby galaxy SDSS J082306.16+033412.1. The limits we describe above on emission from around RGZ J082312.9+033301 would clearly be consistent with a detection at this level. If so, this would reinforce the idea that the radio galaxy host is somewhat dynamically and physically offset from the rest of the environment. Deeper X-ray data are required to investigate this further.

We can conclude, based on the optical and X-ray constraints we have, that the environment of RGZ J082312.9+033301 is consistent with being a rich group or poor cluster of galaxies. We designate this poor cluster as the "Matorny–Terentev Cluster" RGZ-CL J0823.2+0333. Indications of such a cluster have appeared only indirectly in a few references that refer to some of its members as galaxy pairs (Merchán & Zandivarez 2005; Berlind et al. 2006; Wen, Han & Liu 2009; Keel et al. 2013) or to galaxy groups (Tago et al. 2006; Tempel, Tago & Liivamägi 2012).

3.2 Dynamics of RGZ J082312.9+033301

We want to determine if there is a plausible set of jet and medium parameters that could explain the large size and bent radio morphology of RGZ J082312.9+033301. The parameters include the radius of curvature r_c, the radio jet radius r_r, density ratios of the radio jets ρ_r to that of the cluster environment ρ_{ICM}, the velocity of the radio jets v_r, and the velocity of the galaxy with respect to the cluster's barycentre v_g.

The high ratio of the velocity of the WAT host to the velocity dispersion of the cluster discussed above (1100 km s^{-1}/373 km s^{-1} = 2.9, for the galaxies within 20 arcmin) raises the question of whether it could be a background object, and not bound to the cluster. However, as a background object it would not have a significant local thermal plasma to bend the radio structure. Some perspective on this issue comes from the study of the dynamical distribution of X-ray AGN in 26 Local Cluster Substructure Survey (LoCuSS) clusters (Haines et al. 2012). They show that AGN have velocities between one and three times the velocity dispersion of their clusters, with a mean velocity dispersion 1.5 times that of the non-active galaxies. This distribution is indicative of an infalling population, rather than a virialized one. The WAT host is consistent with this behaviour, and might thus be recently encountering the cluster. The spatial offset between the AGN host and the peak of the X-ray emission, if real, would also be consistent with such a picture.

Fig. 2 allows us to place an upper limit on the radius of the radio jets of $r_r \leq 15$ kpc (9 arcsec) if we use the projected size of the knots or hotspots in the FIRST image. We can also estimate the radius of curvature of the entire WAT to $r_c = 345$ kpc by fitting a circle to connect N3 to S2. In order to determine the densities required to produce the observed bending we use a range of density ratios $\rho_r/\rho_{ICM} = 10^{-6}$–$10^{-2}$ (e.g. Douglass et al. 2011) based on our observation of RGZ J082312.9+033301 living in a cluster (Section 3.1). Using Euler's equation (Begelman, Rees & Blandford 1979; Jones & Owen 1979),

$$\frac{\rho_r v_r^2}{r_c} = \frac{\rho_{ICM} v_g^2}{r_r}, \quad (1)$$

and the values above we find that the velocity of the radio jets is in the range $0.005c < v_r < 0.5c$. While this could be suggestive of explaining its bent shape, we note that these are only radial velocities, and to see a significant bend, an appreciable transverse (plane-of-sky) velocity is required. In addition, if the equation of state is relativistic, then the relativistic enthalpy density is more relevant. The bending depends on the ratio of the jet momentum flux and the ram pressure in the putative cross flow (or, more properly, the pressure change across the jet). If we know or can estimate the ratio of the pressures in the jet and the ambient medium, we can write the bending formula (equation 1) in terms of that ratio and the ratio of the jet and cross flow Mach numbers. In this form one finds that NATs require a relatively small Mach number for the jet flow, of typically only a few if the jet and ambient pressures are comparable. In a WAT the jet Mach number would be higher relative to the cross flow Mach number. Future radio and X-ray observations will provide the necessary data to constrain these parameters.

3.3 Possible re-ignition of RGZ J082312.9+033301

We find that RGZ J082312.9+033301 displays an unusual radio structure extending over a large linear size. Typical features of WAT radio galaxies are regions brightening along the jet trails, especially around the bends. The brightening regions extend farther into bright diffuse components that slowly fade away in brightness. However, RGZ J082312.9+033301 shows tightly collimated radio structure throughout its extent (Fig. 2). Here, we speculate if it is possible that the observed bright regions are hotspots typical of FR II radio galaxies rather than knots along the jet paths (Fig. 1).

Table 3. The estimated time-scale for the possible three episodes of formation. We use the estimated jet velocity $v_r = 0.05c$ for these calculations.

Comp.	Separation (kpc)	t_{min} (Myr)
C–N1	79	5
C–S1	126	8
C–N2	294	19
C–S2	312	20
C–N3	592	38
C–S3	538	35

The existence of hotspots could suggest that the WAT is a restarted (double–double) radio galaxy having had two or three episodes of activity during its lifetime.

Assuming the head jet speed is $v = 0.05c$ from the velocity range in Section 3.2, we evaluate the minimum age of the observed radio structures simply as $t_{min} = d/v_r$. In Table 3 we list the separation between components and the estimated time-scale for $z = 0.0897$. We calculate the minimum age of the northern arm (C–N2) as 19 Myr and of the southern arm (C–S2) as 20 Myr. It typically takes between 0.1 and 100 Myr for the radio structures to dissipate once the central AGN engine switches off (e.g. Komissarov & Gubanov 1994; Kaiser, Schoenmakers & Röttgering 2000; Kapińska et al. 2015). With these time-scales one would expect hotspots from previous activity to almost entirely fade away leaving behind diffuse emission of the remnant lobes (N2, S2). Component N2 appears to have features consistent with FR II hotspots while component S2 does not, suggesting that the AGN engine has switched off and the hotspots are beginning to dissipate.

Radio galaxies have been shown to undergo multiple active phases separated by periods of quiescence time when the jet production is shutdown (e.g. Kaiser et al. 2000; Schoenmakers et al. 2000; Saikia & Jamrozy 2009). The dormant/quiescent phase for the AGN may last between 1000 yr and 100 Myr (e.g. Shabala et al. 2008; Kunert-Bajraszewska et al. 2011; Shulevski et al. 2015). The inner components (second phase of AGN activity) may be as young as 5 (C–N1) and 8 Myr (C–S1). The implied dormant phase of the order of 10 Myr would be consistent with typical time-scales for the quiescent phase of radio activity. Therefore, RGZ J082312.9+033301 could have had two episodes of AGN activity.

However, the speculative N3 and S3 components would only work in such a scenario if one considers a much rarer case of an inverted triple–double source. A triple–double is a radio galaxy that displays three episodes of activity; at least one such example is known (Brocksopp et al. 2007). An inverted double–double is a restarted radio galaxy in which the hotspots from the new activity episode were formed farther away from the radio core than the previous activity older material. This may happen if the density of the previous activity plasma has decreased enough for the restarted jets to pass easily through. This scenario would require the dormant stage of the order of 100 Myr and no hotspots formed within components N1, S1, N2, and S2 (Kaiser et al. 2000; Marecki & Szablewski 2009, and references therein). We find no evidence of extended relic radio emission around components N3 and S3, but instead rather compact emission. Therefore, RGZ J082312.9+033301 does not show characteristics of an inverted triple–double source.

All previously discovered double–double radio galaxies display classical straight radio structures (FR II morphology). If RGZ J082312.9+033301 is indeed a restarted radio source, it would pose significant questions as well as constraints on the evolutionary models of restarted radio galaxies (cf. Brocksopp et al. 2007, 2011). To resolve this issue both high resolution high radio frequency, and low radio frequency observations are required, which will allow one to investigate the existence of hotspots and determine the spectral ages of the components. We are currently pursuing observations to address these issues and results will be presented in forthcoming publications.

4 CONCLUSIONS

We presented evidence for a previously unreported poor cluster of galaxies (Matorny–Terentev Cluster, or RGZ-CL J0823.2+0333) discovered through an unusual giant WAT radio galaxy found with the citizen science project Radio Galaxy Zoo (Banfield et al. 2015). The host of RGZ J082312.9+033301 is also known as 2MASX J08231289+0333016 and has been classified by volunteers of Galaxy Zoo 2 (Willett et al. 2013) to be of Hubble type E0. We estimate the 1.4 GHz luminosity density to be $L_{1.4} = 5.5 \times 10^{24}$ W Hz^{-1}. Using the Oxford *Swift* IFU spectrograph on the Palomar 5-m telescope we found RGZ J082312.9+033301 to have a redshift $z = 0.0897 \pm 0.0001$. At this redshift, we find the largest linear size of RGZ J082312.9+033301 to be 0.8 Mpc, measuring 1.1 Mpc along its curved tails making this giant WAT comparable in size to the largest known WAT 4C+47.51.

Investigation of the surround environment through the $N_{1.0}^{-19}$ measurement by Wing & Blanton (2011) indicates that RGZ J082312.9+033301 is located in a cluster near the poor end of the cluster richness spectrum, consistent with Abell's cluster richness classification (Abell, Corwin & Olowin 1989). However, RGZ-CL J0823.2+0333 was not found in the redMaPPer catalogue (Rykoff et al. 2014) and our X-ray analysis indicates that RGZ J082312.9+033301 lives within a rich group rather than a cluster. Thus, combining the radio, optical, and X-ray data we conclude that RGZ J082312.9+033301 lives in an unreported poor cluster of galaxies.

In order to understand the radio morphology of RGZ J082312.9+033301, we have placed limits on the dynamics of the system. We estimate the velocity of RGZ J082312.9+033301 to be $v_g \geq 1100$ km s^{-1} with a jet velocity of $0.005c \leq v_r \leq 0.5c$. Using these values we have shown that RGZ J082312.9+033301 could have multiple retriggering episodes of active phases with a dormant phase on the order of 10 Myr.

The discovery of RGZ J082312.9+033301 shows the benefit of using bent-tail radio sources as beacons of clusters of galaxies. However, the difficulty lies in detecting them in the data of the upcoming radio surveys like EMU, WODAN, and MeerKAT MIGHTEE. Expanding on further citizen science projects building on Radio Galaxy Zoo, or on the future development of machine-learning techniques will be key to locating these bent-tail radio sources to find and study clusters of galaxies.

ACKNOWLEDGEMENTS

This publication has been made possible by the participation of more than 8700 volunteers in the Radio Galaxy Zoo project. Their contributions are individually acknowledged at http://rgzauthors.galaxyzoo.org. We thank M. Chow-Martínez for extracting dynamical parameters using the ROBUST software and Nathan Secrest and Nora Loiseau for information on the *XMM–Newton* data. Parts of this research were conducted by the Australian Research Council Centre of Excellence for All-sky Astrophysics (CAASTRO), through project number CE110001020. OIW acknowledges a Super Science Fellowship from the Australian Research Council. LR, KWW, and TWJ acknowledge partial support from the US National Science Foundation under grant AST-1211595 to the University of Minnesota. MJH acknowledges support from the UK Science and Technology Facilities Council [ST/M001008/1]. GC acknowledges support from STFC grant ST/K005596/1 and SV acknowledges a doctoral studentship supported by STFC grant ST/N504233/1. SSS thanks the Australian Research Council for an Early Career Fellowship DE130101399. NS is the recipient of an Australian Research Council Future Fellowship.

This publication makes use of data products from the *Wide-field Infrared Survey Explorer* and the Very Large Array. The *Wide-field Infrared Survey Explorer* is a joint project of the University of California, Los Angeles, and the Jet Propulsion Laboratory/California Institute of Technology, funded by the National Aeronautics and Space Administration. The National Radio Astronomy Observatory is a facility of the National Science Foundation operated under co-operative agreement by Associated Universities, Inc. This research has made use of the NASA/IPAC Extragalactic Database (NED) which is operated by the Jet Propulsion Laboratory, California Institute of Technology, under contract with the National Aeronautics and Space Administration. The figures in this work made use of ASTROPY, a community-developed core PYTHON package for astronomy (Astropy Collaboration et al. 2013).

REFERENCES

Abell G. O., Corwin H. G., Jr, Olowin R. P., 1989, ApJS, 70, 1
Adelman-McCarthy J. K. et al., 2006, ApJS, 162, 38
Ahn C. P. et al., 2014, ApJS, 211, 17
Alam S. et al., 2015, ApJS, 219, 12
Astropy Collaboration et al., 2013, A&A, 558, A33
Banfield J. K. et al., 2015, MNRAS, 453, 2326
Becker R. H., White R. L., Helfand D. J., 1995, ApJ, 450, 559
Becker M. R. et al., 2007, ApJ, 669, 905
Beers T. C., Flynn K., Gebhardt K., 1990, AJ, 100, 32
Begelman M. C., Rees M. J., Blandford R. D., 1979, Nature, 279, 770
Berlind A. A. et al., 2006, ApJS, 167, 1
Best P. N., 2009, Astron. Nachr., 330, 184
Brocksopp C., Kaiser C. R., Schoenmakers A. P., de Bruyn A. G., 2007, MNRAS, 382, 1019
Brocksopp C., Kaiser C. R., Schoenmakers A. P., de Bruyn A. G., 2011, MNRAS, 410, 484
Condon J. J., Cotton W. D., Greisen E. W., Yin Q. F., Perley R. A., Taylor G. B., Broderick J. J., 1998, AJ, 115, 1693
Coziol R., Andernach H., Caretta C. A., Alamo-Martínez K. A., Tago E., 2009, AJ, 137, 4795
Douglass E. M., Blanton E. L., Clarke T. E., Randall S. W., Wing J. D., 2011, ApJ, 743, 199
Eilek J. A., Burns J. O., O'Dea C. P., Owen F. N., 1984, ApJ, 278, 37
Fanaroff B. L., Riley J. M., 1974, MNRAS, 167, 31p
Giacintucci S., Venturi T., 2009, A&A, 505, 55
Green D. A., 2011, Bull. Astron. Soc. India, 39, 289
Haines C. P. et al., 2012, ApJ, 754, 97
Hao J. et al., 2010, ApJS, 191, 254
Hardcastle M. J., 1998, MNRAS, 298, 569
Hardcastle M. J., Sakelliou I., Worrall D. M., 2005, MNRAS, 359, 1007
Hardcastle M. J., Evans D. A., Croston J. H., 2009, MNRAS, 396, 1929
Helsdon S. F., Ponman T. J., 2000, MNRAS, 315, 356
Ineson J., Croston J. H., Hardcastle M. J., Kraft R. P., Evans D. A., Jarvis M., 2015, MNRAS, 453, 2682
Jarvis M. J., 2012, African Skies, 16, 44
Jetha N. N., Hardcastle M. J., Sakelliou I., 2006, MNRAS, 368, 609
Jones T. W., Owen F. N., 1979, ApJ, 234, 818

Kaiser C. R., Schoenmakers A. P., Röttgering H. J. A., 2000, MNRAS, 315, 381
Kapińska A. D., Hardcastle M., Jackson C., An T., Baan W., Jarvis M., 2015, in Proceedings of Advancing Astrophysics with the Square Kilometre Array (AASKA14). Online at http://pos.sissa.it/cgi-bin/reader/conf.cgi?confid=215, id. 173
Katz-Stone D. M., Rudnick L., Butenhoff C., O'Donoghue A. A., 1999, ApJ, 516, 716
Keel W. C., Manning A. M., Holwerda B. W., Mezzoprete M., Lintott C. J., Schawinski K., Gay P., Masters K. L., 2013, PASP, 125, 2
Komissarov S. S., Gubanov A. G., 1994, A&A, 285, 27
Kunert-Bajraszewska M., Janiuk A., Siemiginowska A., Gawroński M., 2011, in Romero G. E., Sunyaev R. A., Belloni T., eds, Proc. IAU Symp. 275, Jets at All Scales. Cambridge Univ. Press, Cambridge, p. 180
Lupton R., Blanton M. R., Fekete G., Hogg D. W., O'Mullane W., Szalay A., Wherry N., 2004, PASP, 116, 133
Marecki A., Szablewski M., 2009, A&A, 506, L33
Mendygral P. J., Jones T. W., Dolag K., 2012, ApJ, 750, 166
Merchán M. E., Zandivarez A., 2005, ApJ, 630, 759
Norris R. P. et al., 2011, Publ. Astron. Soc. Aust., 28, 215
O'Donoghue A. A., Eilek J. A., Owen F. N., 1993, ApJ, 408, 428
Owen F. N., Ledlow M. J., 1994, in Bicknell G. V., Dopita M. A., Quinn P. J., eds, ASP Conf. Ser. Vol. 54, The First Stromlo Symposium: The Physics of Active Galaxies. Astron. Soc. Pac., San Francisco, p. 319
Owen F. N., Rudnick L., 1976, ApJ, 205, L1
Pinkney J., Burns J. O., Hill J. M., 1994, AJ, 108, 2031
Röttgering H. et al., 2011, J. Astrophys. Astron., 32, 557
Rudnick L., Owen F. N., 1976, ApJ, 203, L107
Rykoff E. S. et al., 2014, ApJ, 785, 104
Sadler E. M., Ekers R. D., Mahony E. K., Mauch T., Murphy T., 2014, MNRAS, 438, 796
Saikia D. J., Jamrozy M., 2009, Bull. Astron. Soc. India, 37, 63
Sakelliou I., Merrifield M. R., McHardy I. M., 1996, MNRAS, 283, 673
Schoenmakers A. P., de Bruyn A. G., Röttgering H. J. A., van der Laan H., Kaiser C. R., 2000, MNRAS, 315, 371
Shabala S. S., Ash S., Alexander P., Riley J. M., 2008, MNRAS, 388, 625
Shulevski A. et al., 2015, A&A, 579, A27
Tago E. et al., 2006, Astron. Nachr., 327, 365
Tempel E., Tago E., Liivamägi L. J., 2012, A&A, 540, A106
Thatte N. et al., 2010, Proc. SPIE, 7735, 77357Y
Wen Z. L., Han J. L., Liu F. S., 2009, ApJS, 183, 197
White R. L., Becker R. H., Helfand D. J., Gregg M. D., 1997, ApJ, 475, 479
Willett K. W. et al., 2013, MNRAS, 435, 2835
Wing J. D., Blanton E. L., 2011, AJ, 141, 88
Wright E. L., 2006, PASP, 118, 1711
Wright E. L. et al., 2010, AJ, 140, 1868

This paper has been typeset from a TEX/LATEX file prepared by the author.